Crack Detection through the Change in the Normalized Frequency Shape

Mustapha Dahak [1],*, Noureddine Touat [1] and Tarak Benkedjouh [2]

[1]   Applied Mechanics Laboratory, University of Science and Technology Houari Boumediene, 16111 Algiers, Algeria; ntouat@usthb.dz
[2]   Laboratoire de Mécanique des Structures, Ecole Militaire Polytechnique, Bordj El Bahri, 16111 Algiers, Algeria; bktarek@gmail.com
*   Correspondence: mdahak@usthb.dz; Tel.: +213-662838306

Abstract: The objective of this work is to use natural frequencies for the localization and quantification of cracks in beams. First, to study the effect of the crack on natural frequencies, a finite element model of Euler–Bernoulli is presented. Concerning the damaged element, the stiffness matrix is calculated by the theory of fracture mechanics, by inverting the flexibility matrix. Then, in order to detect damage, we are going to show that the shape given by the change in the natural frequencies is as function of the damage position only. Thus, the crack is located by the correlation between the shape of the measured frequencies and those obtained by the finite elements, where the position that gives the calculated shape which is the most similar to the measured one, indicates the crack position. After the localization, an inverse method will be applied to quantify the damage. Finally, an experimental application is presented to show the real applicability of the method, in which the crack is introduced by using an Electrical Discharge Machining. The results confirm the applicability of the method for the localization and the quantification of cracks.

1. Introduction

Due to mechanical vibration, environmental attack and long-term service, etc., mechanical structures may be damaged. Therefore, an early detection of these defects seems crucial for safety and economic reasons, as their detection can significantly extend the life of the structure, which increases its reliability at the same time. In recent years, several studies have been presented to detect the damage through the change in dynamic and static properties. Andreaus and Casini [1] presented a multiple damaged detection method based on static deflection. The basic idea of the method is the fact that the crack produces a local singularity in the displacement response which can be detected by a wavelet analysis. However, the drawback of the static damage identification methods is that the static response provides less information as compared to dynamic response. In the vibration-based detection methods, the damage can be detected through modifications in the linear response (modal parameters) or by the occurrence of nonlinear effects [2–4]. A detailed review of the previous researches on the vibration-based detection methods are given in [5–7]. Cao et al. [8] has shown that the damping is the least applied dynamic parameters for the damage identification, because of the difficulty involved in traditional measurement. However, the modes shapes were widely used for the damage detection because of their sensitivity in each position of the structure, which makes them the most appropriate to localize the damage. Homaei et al. [9] proposed a criterion named "Multiple Damage Localization Index Based on Mode Shapes" to localize the damage by combining the mode shapes of both damaged

and undamaged structures. Ravi Prakash Babu et al. [10] showed that by deriving the mode shape, the damage effect increases. Then, the authors proposed using the curvature mode shape for the damage localization. Finally, the authors concluded that the curvature mode shape is more sensitive than the mode shape. Cao et al. [11] indicated that the disadvantage in deriving the mode shape is the fact that it amplifies the noise. Therefore, the authors proposed to improve the curvature with wavelet transform and a Teager energy operator. Further, in order to improve the results of damage detection, Yazdanpanah et al. [12] proposed utilizing both the mode shape slope and mode shape curvature. Rucevskis et al. [13,14] demonstrated that the data of the intact structure have a smooth surface. Thus, the authors proposed a method without baseline data by replacing the curvature of the healthy structure with a smoothed polynomial. Another method without baseline data was proposed by Zhong et al. and Jaiswal et al. [15,16]. The method is based on the application of the wavelet transform to the curvature mode shape. Though, the mode shape and its derivatives are most appropriate to localize the damage, because they are less effective for the damage quantification. Xiang et al. [17] proposed a hybrid method using mode shape and natural frequency measurements. First, the damage is localized using the mode shape. Then, the crack depth is estimated using the natural frequency as inputs.

The other modal parameter is the natural frequency. According to Fan and Qiao [6], the natural frequency is affected by the temperature variations, and its application is limited to a controlled laboratory condition. However, that did not discourage other researchers, due to its ease of measurement and the cheap experimental procedure. According to Doebling et al. [18], the authors in (Lifshitz and Rotem [19]) presented the first method of detecting damage using vibratory measurements. The authors used the shift in natural frequencies, through changes in Young's modulus. Salawu [20] provided detailed review of studies on damage identification methods based on natural frequency. Dahak et al. [21] showed that if one of the natural frequencies remains unchanged, the crack is located in the vibration nodes of the corresponding mode. Thus, the authors used the classification of the first four normalized frequencies to distinguish the node and locate the damage. Banerjee et al. [22] proposed a frequency contours method. The method consists of plotting contours of the first three frequencies with respect to crack depth and position, and the intersection of plotted contours gives a crack position and size. Recently, Dahak et al. [23] simplified the method by using a curvature mode shape rather than calculating the frequencies versus the crack position and depth. A key limitation of the frequency contours method is that it detects only a single damage. In order to detect a double crack, Mazanoglu et al. [24] combined it with an algorithm. Also, many researchers have considered the damage identification as an optimization problem. The position and depth of the crack are considered as design variables. In this area, there are the bee algorithm [25], the modified Cuckoo optimization algorithm [26], artificial neural networks [27], and genetic algorithms [28]. Recently, Boubakir et al. [29] improved the accelerated random search algorithm of (Touat et al. [30]) and applied it for the detection of damage in the beams. However, the disadvantage of these methods is in the search for the position and the depth at the same time. Therefore, the objective of this work is to develop a new method to detect crack in beam in two steps. First, estimating the crack position and then quantifying it.

In this framework, we show that the shape given by the normalized natural frequencies changes only according to the damage location. Thus, the damage is localized by the correlation between the shape of the measured normalized frequencies and those obtained by the finite elements, where the position that gives the calculated shape, which is the most similar to the measured one, indicates the crack position. After the localization, an inverse method will be applied in order to quantify the damage.

2. Finite Element Formulation

2.1. Intact Element

Considering a Euler–Bernoulli beam having length L, depth h and width w. The elemental mass matrix (m_e) and elemental stiffness matrix (k_e) without damage are expressed as follows:

$$m_e = \frac{\rho A l_e}{420} \begin{bmatrix} 156 & 22l_e & 54 & -13l_e \\ 22l_e & 4l_e{}^2 & 13l_e & -3l_e{}^2 \\ 54 & 13l_e & 12 & -22l_e \\ -13l_e & -3l_e{}^2 & -22l_e & 4l_e{}^2 \end{bmatrix} \tag{1}$$

$$k_e = \frac{EI}{l_e{}^3} \begin{bmatrix} 12 & 6l_e & -12 & 6l_e \\ 6l_e & 4l_e{}^2 & -6l_e & 2l_e{}^2 \\ -12 & -6l_e & 12 & -6l_e \\ 6l_e & 2l_e{}^2 & -6l_e & 4l_e{}^2 \end{bmatrix} \tag{2}$$

where A, E, l_e, I and ρ are the area of the cross section, Young modulus, element length, moment of inertia and material density, respectively.

2.2. Damaged Element

Considering a beam with a crack of depth h_d at the position l_d from the fixed end. The crack is considered as transversal crack under bending and shearing forces. The local stiffness is reduced whenever damage occurs in the structure. By applying the principle of virtual work [31] and the equilibrium condition of the cracked element, the damaged elemental stiffness matrix (k_{ed}) is given from the inverse of the flexibility matrix [32]:

$$\left[k_{ed(i,j)} \right] = \left[T_{(i,k)} \right]^t \left[C^{int}{}_{(k,k)} + C^d{}_{(k,k)} \right]^{-1} \left[T_{(k,j)} \right] \tag{3}$$
$$i, j = 1:4; \; k = 1:2$$

where T, C^{int} and C^d are the transformation matrix, the intact flexibility matrix and the additional flexibility matrix due to the presence of the crack, respectively. The upper index "t" indicates the transpose and the upper index "-1" indicates the inverse of the matrix.

The transformation matrix $[T]$ is given as:

$$[T]^t = \begin{bmatrix} -1 & -le & 1 & 0 \\ 0 & -1 & 0 & 1 \end{bmatrix}^t \tag{4}$$

The flexibility matrix of the intact beam (C^{int}) is:

$$C^{int} = \begin{bmatrix} \frac{(l_e)^3}{3EI} & \frac{(l_e)^2}{2EI} \\ \frac{(l_e)^2}{2EI} & \frac{l_e}{EI} \end{bmatrix} \tag{5}$$

The elements of the flexibility matrix (C^d) are given by [32]:

$$C_{11}^d = \frac{(1-v^2)}{E} \frac{2\pi}{w} \left[\frac{9\, l_e^2}{h^2} \times \int_0^{\overline{h_d}} \overline{h_d}\, F_1^2\left(\overline{h_d}\right) d\overline{h_d} + \int_0^{\overline{h_d}} \overline{h_d}\, F_2^2\left(\overline{h_d}\right) d\overline{h_d} \right] \tag{6}$$

$$C_{22}^d = \frac{(1-v^2)}{E} \frac{72\pi}{wh^2} \int_0^{\overline{h_c}} \overline{h_d}\, F_1^2\left(\overline{h_d}\right) d\overline{h_d} \tag{7}$$

$$C_{21}^d = C_{12}^d = \frac{(1 - v^2)}{E} \frac{36\pi\, l_e}{wh^2} \int_0^{\overline{h_d}} \overline{h_d}\, F_1^2\left(\overline{h_d}\right)\, d\overline{h_d} \tag{8}$$

where v is the ratio of Poisson and $\overline{h_d}$ is the normalized crack depth expressed as:

$$\overline{h_d} = \frac{h_d}{h} \tag{9}$$

F_1 and F_2 are correction factors given as [33]:

$$F_1\left(\overline{h_d}\right) = \frac{\left[0.199\left(1 - \sin\left(\frac{\overline{h_d}\pi}{2}\right)\right)^4 + 0.923\right]}{\cos\left(\frac{\overline{h_d}\pi}{2}\right)} \times \sqrt{\frac{\tan\left(\frac{\overline{h_d}\pi}{2}\right)}{\left(\frac{\overline{h_d}\pi}{2}\right)}} \tag{10}$$

$$F_2\left(\overline{h_d}\right) = \frac{\left[0.18\left(\overline{h_d}\right)^3 + 0.85\left(\overline{h_d}\right)^2 - 0.561\left(\overline{h_d}\right) + 1.122\right]}{\sqrt{1 - \overline{h_d}}} \tag{11}$$

3. Crack Detection Method

3.1. Crack Localization

Considering the normalized natural frequency of mode i given as:

$$df_i = \frac{f_i^{damaged}}{f_i^{intact}} \tag{12}$$

where, $\left(f_i^{damaged}\right)$ and $\left(f_i^{intact}\right)$ are the frequency of the damaged structure and the frequency of the intact structure, respectively.

To study the effect of the crack on the normalized natural frequencies, consider a cantilever beam in Table 1 with uniform rectangular cross section and an isotropic material. Using the finite element method presented in the previous section and the MATLAB code, the beam is discretized into 100 elements.

Table 1. The dimensions and material of the beam.

Boundary Conditions	Material				Dimensions		
	Material	E (GPa)	ρ (kg/m^3)	v	L (mm)	w (mm)	h (mm)
Cantilever	Zicral	72	2810	0.35	600	26	7.6

Figure 1 represents the variation of the first four normalized natural frequencies of the cantilever beam (Table 1) as function of the position and the depth of the crack. In this figure, we can see that the frequencies are influenced by the position and the depth of the crack. Therefore, cracks with different depths and positions can cause the same change in one frequency. But, there is only one crack that can produce the same change in several frequencies. Thus, by looking for data that change only according to the crack position, the damage can be located by the correlation between the measured and the calculated data, by varying only the crack position, instead of varying the two parameters.
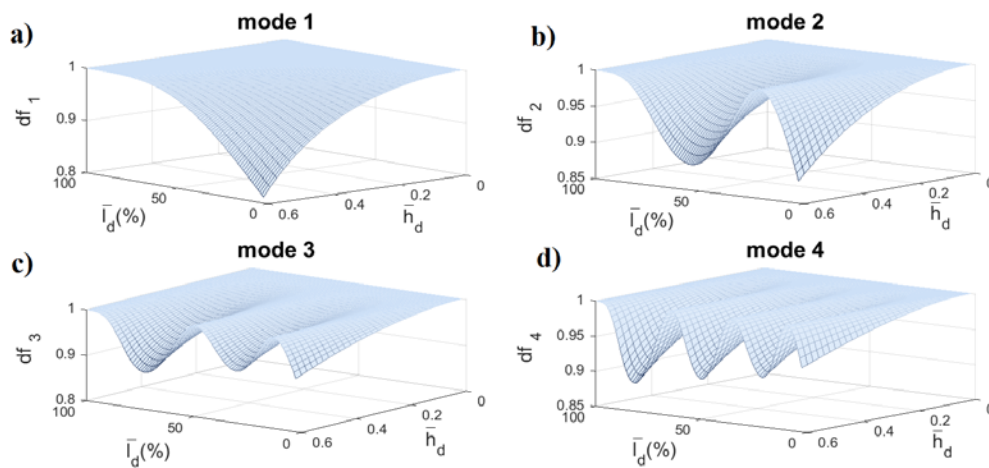
Figure 1. Normalized Frequencies as function of the crack position and its depth; (**a**) 1st mode; (**b**) 2nd mode; (**c**) 3rd mode; and (**d**) 4th mode.

Figure 2 shows the shape of the first four normalized frequencies (*df*) for different crack positions (for a fixed depth of 3 mm). We can notice that the forms given by *df* change according to the crack position, where each position gives a specific shape. According to Dahak et al. [23], the presence of crack produces a loss of stored strain energy, and this loss of stored energy changes as function of the value of the curvature mode shape at the crack position. In summary, each frequency changes according to its mode shape displacement at the position of the crack, which explains why each crack position gives different forms of *df*. Thus, the shape given by the frequencies is characterized by the crack position, and the crack depth just amplifies it. For example, Figure 3 shows the shape of the first four normalized frequencies for different crack depths (at the fixed position $\bar{l}_d = 50\%$). We can notice that the shapes given by *df* is the same for each crack depths.
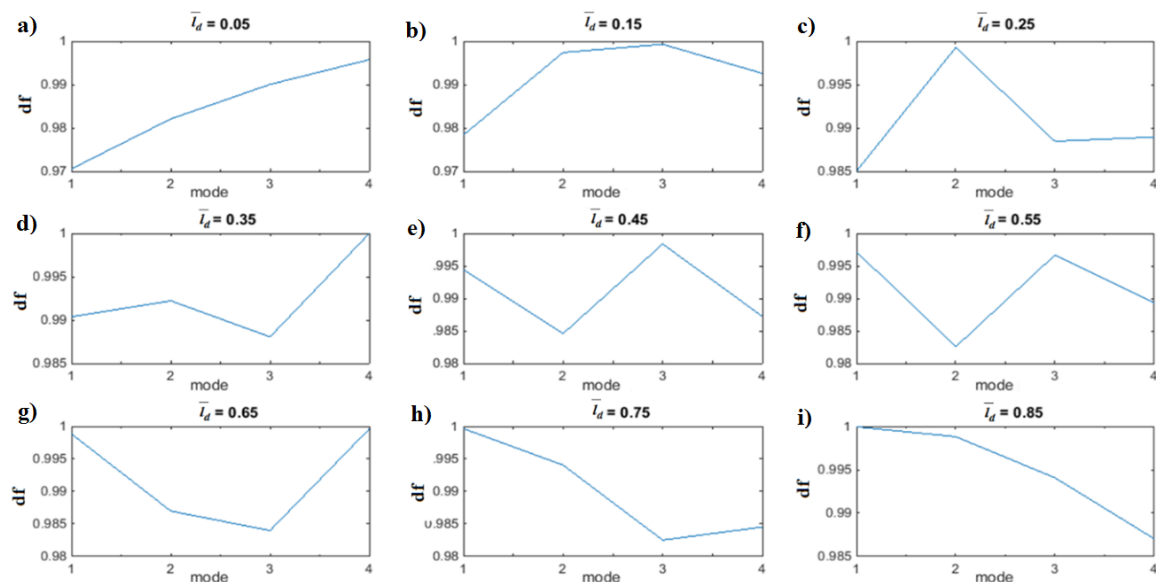

Figure 2. The shape of the first four normalized frequencies for different crack positions. (**a**) $\bar{l}_d = 0.05$, (**b**) $\bar{l}_d = 0.15$, (**c**) $\bar{l}_d = 0.25$, (**d**) $\bar{l}_d = 0.35$, (**e**) $\bar{l}_d = 0.45$, (**f**) $\bar{l}_d = 0.55$, (**g**) $\bar{l}_d = 0.65$, (**h**) $\bar{l}_d = 0.75$ and (**i**) $\bar{l}_d = 0.85$.
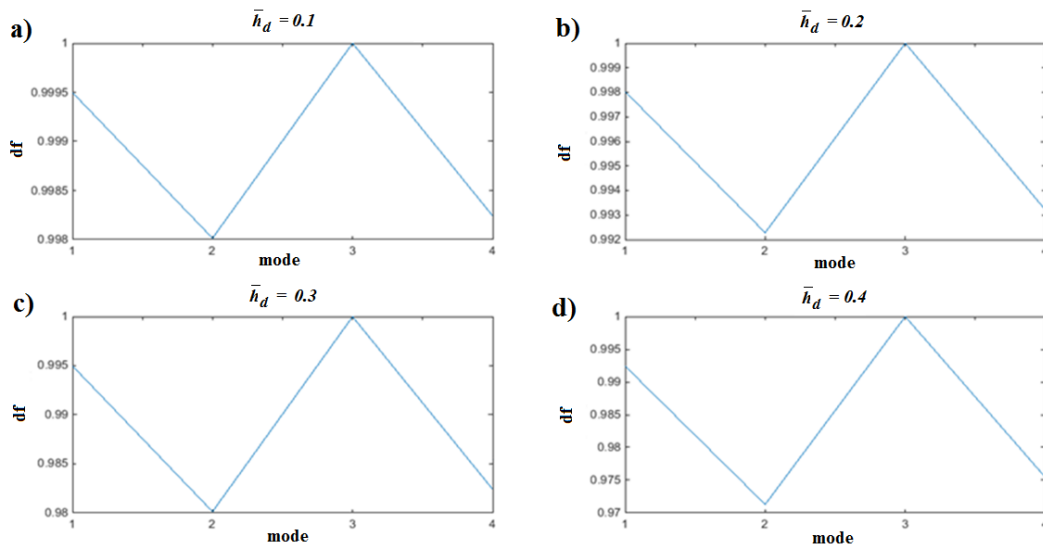
Figure 3. The shape of the first four normalized frequencies for the crack position $\bar{l}_d$ = 50%. (**a**) $\bar{h}_d$ = 10%, (**b**) $\bar{h}_d$ = 20%, (**c**) $\bar{h}_d$ = 30% and (**d**) $\bar{h}_d$ = 40%.

Consequently, the damage can be located by the correlation between the measured shape and the calculated one. But the only problem is that the scale of this shape changes according to the crack depth (for example: in Figure 3: a—Fr2 = 0.998, b—Fr2 = 0.992, c—Fr2 = 0.98, d—Fr2 = 0.97). Thus, by normalizing this shape to be a function of only the crack position, we can locate the damage by the correlation between the measured normalized shape and the calculated one, by varying only the crack position. Therefore, the normalization of the frequencies shape is given as

$$\Delta f_{(1:4)} = \left(\frac{df_{(1:4)}}{df_{(2)} - df_{(1)}} - \frac{df_{(1)}}{df_{(2)} - df_{(1)}} \right) \times sign\left(\frac{df_{(1)}}{df_{(2)}} - 1 \right) \tag{13}$$

Figure 4 shows the frequencies shape normalized by Equation (13) for different crack depths. We can notice that the normalized frequencies shape does not change as a function of the crack depths. Therefore, in order to locate the damage, the normalized frequencies shape is calculated for different crack positions, and the position that gives the calculated shape, which is the most similar to the measured one, indicates the crack position.
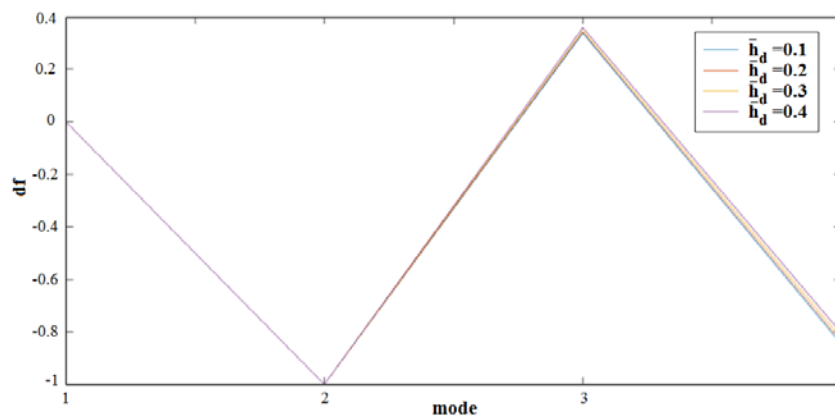

Figure 4. The normalized shape for different crack depths.

For example, considering The beam damaged with a crack at the location of 300 mm. in order to localize the crack, the normalized frequencies shape is calculated for different crack position with

a step of 60 mm. The estimated normalized shapes for each supposed crack position are represented in blue and the real ones in red (Figure 5). Therefore, it is clear that the two vectors coincide at the position of 300 mm, which is the real crack position.
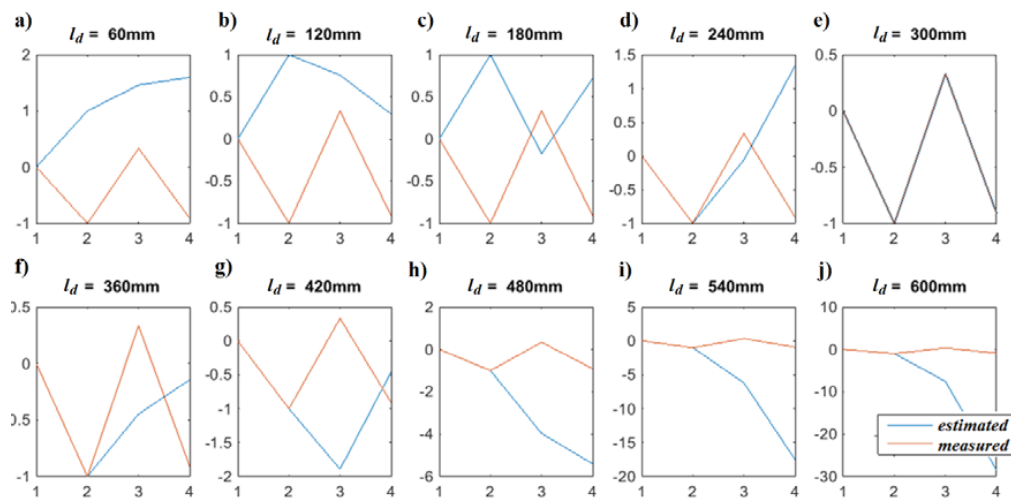

Figure 5. Crack localization. (**a**) l_d = 60 mm, (**b**) l_d = 120 mm, (**c**) l_d = 60 mm, (**d**) l_d = 180 mm, (**e**) l_d = 300 mm, (**f**) l_d = 360 mm, (**g**) l_d = 420 mm, (**h**) l_d = 480 mm, (**i**) l_d = 540 mm, (**j**) l_d = 600 mm.

It is noted that the frequency reduction changes due to boundary condition; consequently, the shapes of the normalized frequencies are different for each boundary condition. Therefore, the consideration of boundary conditions is crucial for the correlation between the measured and the calculated data.

3.2. Crack Quantification

After the location of the crack, an inverse method inspired from the literature is used to estimate the crack depth [34]. First, the localized crack position is used to plot one of the frequencies as function of the crack depth. Then, the projection of the measured frequency gives the crack depth.

It is noted that any modal frequency can be used for the damage quantification. But it is recommended to use the frequency that has undergone the greatest decrease because it gives more readable results.

For example, for the previous case, the frequency of the second mode has undergone the greatest decrease (df_2 = 0.9646). Thus, this frequency is ploted as function of the the crack depth with a step of 1% (see Figure 6), and the crack depth ratio is estimated to be 50% of the beam depth.
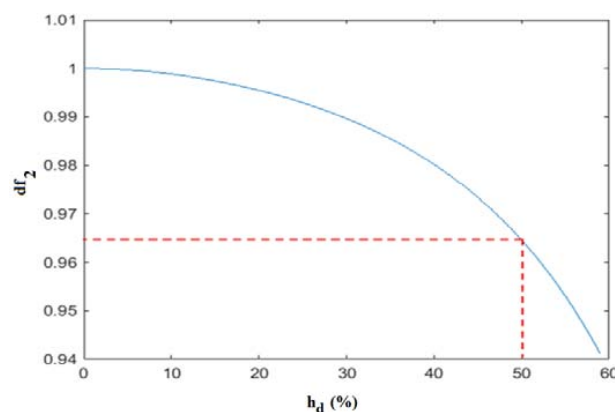

Figure 6. Crack quantification.

4. Numerical Application

In this section, the applicability of the proposed method is shown by using numerical data simulated with "ANSYS-APDL 14.0" commercial software under free vibration. Six cases of damage are applied, where the crack position and its depth vary in each case. The dimensions and material of the cantilever beam are represented in Table 1. First, points are created to construct the area of the beam with a U-shaped edge crack on its top surface. The crack width is 0.1 mm. A six nodes triangular element "PLANE2" is selected to model the beam. Then, the beam is discritized into 2389 triangular elements with 5352 nodes. After meshing, the cantilever boundary condition is applied, by constraining all degrees of freedoms of the nodes located at the left end of the beam. Finally, "BLOCK LANCZOS" mode extraction method is used to calculate the natural frequencies of the beam.

The first four frequencies calculated for each case are represented in Table 2. The case 0 indicates the frequencies of the intact beam. Using these frequencies and by following the approach presented in Section 3, the crack position is varied with a step of 1% (6 mm) and the crack positions are localized by the correlation (Figure 7). Then, the crack is quantified, using the inverse method by varying the crack depth with a step of 1% (Figure 8).

Table 2. Natural frequencies of the numerical application.

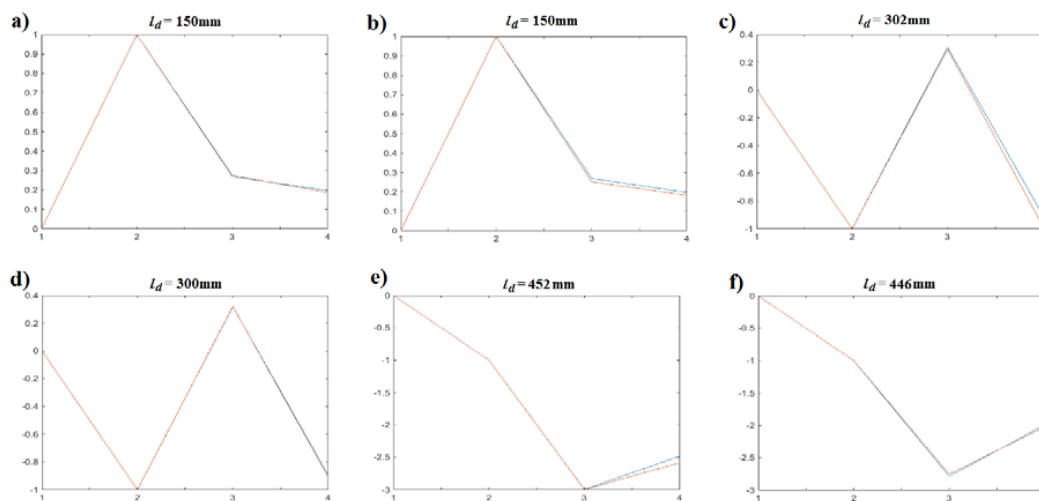|	Cracks		Natural Frequencies			
Case	l_d (mm)	$\overline{h_d}$ (%)	f_1	f_2	f_3	f_4
0	0	0	17.265	108.11	302.34	591.42
1	150	20	17.185	108.09	301.27	589.05
2	150	40	16.911	108.02	297.64	581.41
3	300	15	17.253	107.78	302.34	589.64
4	300	50	17.09	103.58	302.34	568.64
5	450	30	17.263	107.64	298.47	584.89
6	450	60	17.241	105.04	279.46	558.25

Figure 7. Crack localization for the numerical application. (**a**) 1st case; (**b**) 2nd case; (**c**) 3rd case; (**d**) 4th case; (**e**) 5th case and (**f**) 6th case.

The results of the localization and quantification of the crack are shown in Table 3. These results show that the estimated values are closed to the exact ones with an error between 0 and 0.67% for the localization and an error between 1.27% and 2.86% for the quantification. In conclusion, the method can be applied to locate and quantify the cracks in beams.
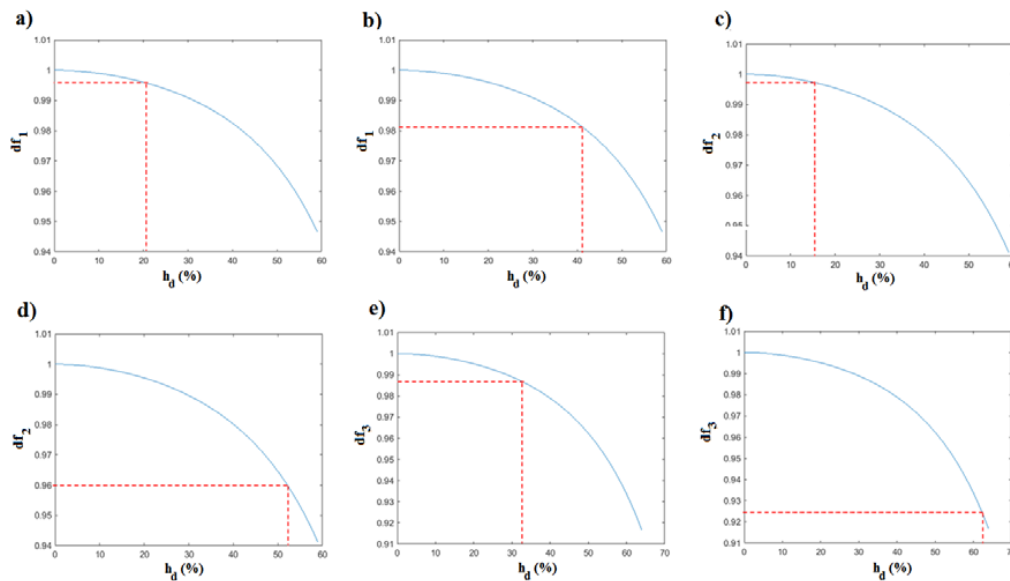
Figure 8. Crack quantification for the numerical application. (**a**) 1st case; (**b**) 2nd case; (**c**) 3rd case; (**d**) 4th case; (**e**) 5th case and (**f**) 6th case.

Table 3. Damage detection for the numerical application.

Case	l_d (mm)	Error (%)	$\overline{h_d}$ (%)	Error (%)
1	150	0	21.47	1.47
2	150	0	42.62	1.62
3	302	0.33	16.27	1.27
4	300	0	52.86	2.86
5	452	0.33	32.51	2.51
6	446	0.67	62.17	2.17

5. Experimental Application

To verify the applicability of the crack detection method, an experimental application has been conducted. The test specimen is a cantilever beam made of aluminum alloy type Zicral (7075). The dimensions, the mechanical properties and the boundary conditions of the beam were chosen exactly similar to those described in the numerical study (Table 1). Figure 9 shows the experimental setup conducted in this study (Brüel and Kjær brand). The cantilever beam is stimulated by an impact hammer (Type 8206-001) which produces a force and measures it at the same time. An accelerometer (Type 4507-B-004) is used to capture the data, which is studied with data acquisition (Type 3560C) and Vold–Kalman filter connected to the computer. The measurement software (pulse labshop) is used to extract the natural frequencies using fast Fourier transform within a frequency range of 0–2 kHz for sampling rate of 6400 points.

First, the intact beam has been tested. Then, the crack has been introduced in the lateral axis by using a wire-cut electro-erosion machine (Figure 10). The first crack is located at the position l_{d1} = 57 mm with a half-width of the beam. For the second case, the beam with the first crack is considered as an undamaged beam and a second crack has been introduced at the location of l_{d2} = 330 mm.

It is noted that the boundary condition before and after the crack creation would be slightly changed because the beam is moved to the cutting machine and reinstalled for the data acquisition. However, the authors have tried to minimize these changes in the boundary condition by taking some benchmarks such as measuring the clamping force of the fixed boundary condition by a torque wrench;

also, we have put an obstacle to mark the location of the embedding. But even that is not enough and there is an irregularity which causes an additional error in the estimation results.
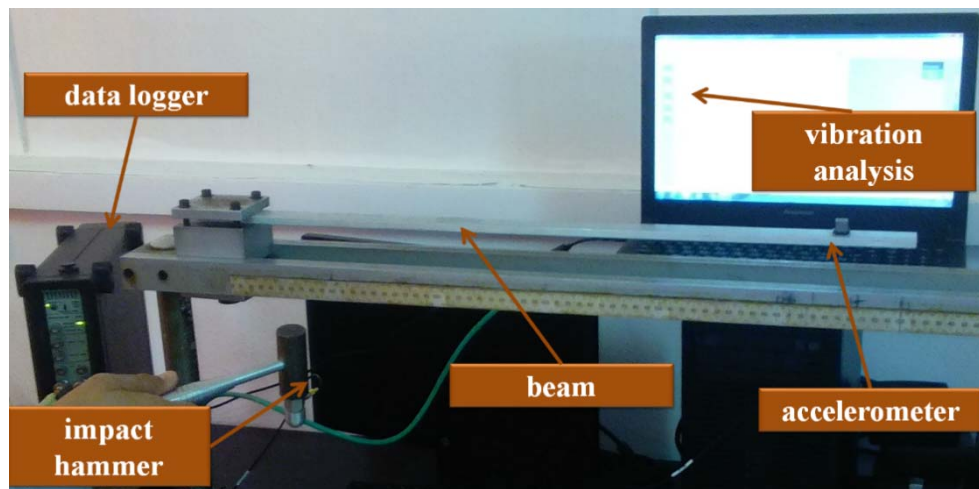

Figure 9. Experimental set-up.

Figure 10. Crack Creation with a wire-cut electro-erosion machine.

The measured frequencies are shown in Table 4, where the "case 0" represents the frequencies of the intact beam, the "case 1" represents the frequencies of the beam with the first crack and the "case 2" represents the frequencies of the beam with the two cracks.

Table 4. The measured frequencies in the experimental application.

Mode No.	Case 0 (Intact Beam)	Case 1 (First Crack)		Case 2 (Second Crack)	
	Frequency (Hz)	Frequency (Hz)	Normalized Frequency	Frequency (Hz)	Normalized Frequency
1	16.17	15.67	0.9691	15.57	0.9936
2	102.79	101.42	0.9867	99.11	0.9772
3	297.32	296.13	0.9960	294.15	0.9933
4	601.79	601.66	0.9998	591.26	0.9827

Using these frequencies and by following the approach presented in Section 3, the crack positions are localized by the correlation (Figure 11). Then, the crack depth is quantified using the inverse method (Figure 12).
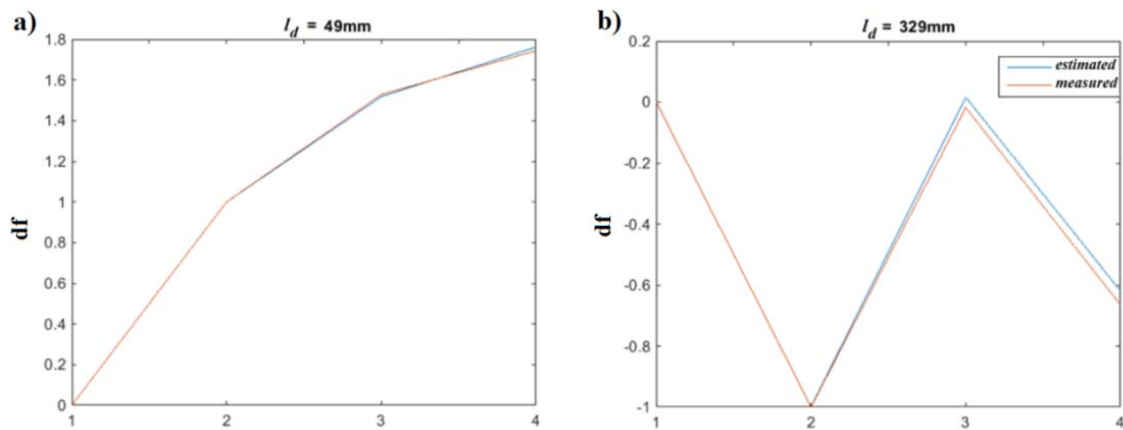
Figure 11. Crack localization for the experimental application. (**a**) 1st case; (**b**) 2nd case.
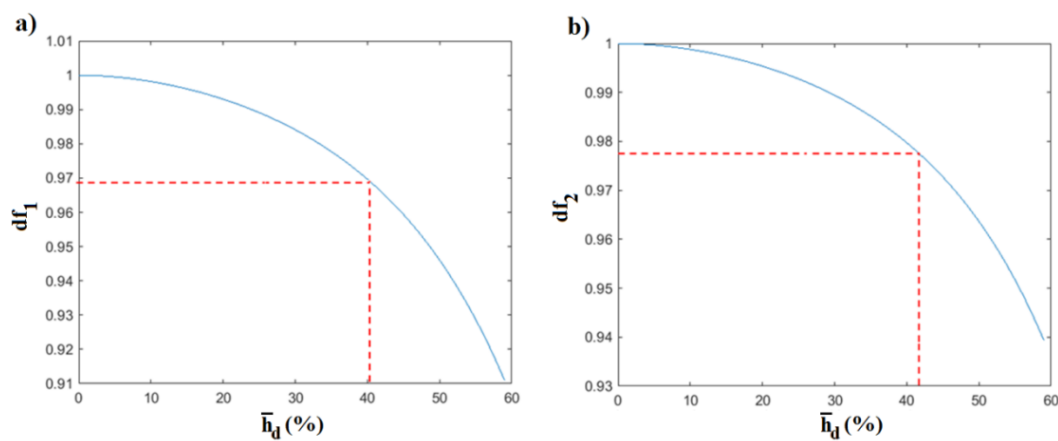

Figure 12. Crack quantification for the experimental application. (**a**) 1st case; (**b**) 2nd case.

The results of the localization and quantification of the crack are shown in Table 5. The results show that the estimated values are closed to the exact ones with an error between 0.16% and 1.33% for the localization and an error between 8.06% and 9.72% for the quantification.

Table 5. Crack detection for the experimental application.

Case	l_d (mm)	Error (%)	$\overline{h_d}$ (%)	Error (%)
1	49	1.33	40.28	9.72
2	329	0.16	41.94	8.06

We can conclude that the estimated results are still admissible compared to those in the literature and some errors are inevitable, first, because of the measurement noise. Then, because the fixed boundary condition is very difficult to achieve in the experimental set-up and would be slightly changed, when the beam is moved to the cutting machine and reinstalled for the data acquisition.

6. Conclusions

A new method to locate and quantify cracks in beams has been presented in this work. The vibratory behaviour of the beam has been modelled using a finite element model of Euler Bernoulli. Concerning the damaged element, the stiffness matrix is calculated by the theory of fracture mechanics, as an inverse of the flexibility matrix.

In order to detect the damage, it has been shown that the shape given by the change in the natural frequencies is as function of the damage position only. Thus, the crack is located by the correlation between the shape of the measured frequencies and those obtained by the finite elements, where the position that gives the calculated shape, which is the most similar to the measured one, indicates the crack position. After the localization, an inverse method is applied to quantify the damage.

Numerical studies by ANSYS APDL and an experimental application have been conducted to test the integrity of the method. The results show that the estimated values are closed to the exact ones with an error less than 1.5% for the localization and less than 10% for the quantification. We can conclude that the estimated results are still admissible.

Finally, it can be concluded that the method has been validated for the damage detection in the cantilever beams, and the same concept can be used to detect damage in other boundary conditions. Therefore, the consideration of boundary conditions is crucial for the correlation between the measured and the calculated data.

References

1. Andreaus, U.; Casini, P. Identification of Multiple Open and Fatigue Cracks in Beam-like Structures Using Wavelets on Deflection Signals. *Contin. Mech. Thermodyn.* **2016**, *28*, 361–378. [CrossRef]
2. Al-Shudeifat, M.A.; Butcher, E.A. On the Dynamics of a Beam with Switching Crack and Damaged Boundaries. *J. Vib. Control* **2013**, *19*, 30–46. [CrossRef]
3. Cole, D.P.; Habtour, E.M.; Sano, T.; Fudger, S.J.; Grendahl, S.M.; Dasgupta, A. Local Mechanical Behavior of Steel Exposed to Nonlinear Harmonic Oscillation. *Exp. Mech.* **2017**, *57*, 1027–1035. [CrossRef]
4. Neves, A.C.; Simões, F.M.F.; Pinto da Costa, A. Vibrations of Cracked Beams: Discrete Mass and Stiffness Models. *Comput. Struct.* **2016**, *168*, 68–77. [CrossRef]
5. Das, S.; Saha, P.; Patro, S.K. Vibration-based damage detection techniques used for health monitoring of structures: A review. *J. Civ. Struct. Health Monit.* **2016**, *6*, 477–507. [CrossRef]
6. Fan, W.; Qiao, P. Vibration-based damage identification methods: A review and comparative study. *Struct. Health Monit.* **2011**, *10*, 83–111. [CrossRef]
7. Jassim, Z.A.; Ali, N.N.; Mustapha, F.; Abdul Jalil, N.A. A review on the vibration analysis for a damage occurrence of a cantilever beam. *Eng. Fail. Anal.* **2013**, *31*, 442–461. [CrossRef]
8. Cao, M.S.; Sha, G.G.; Gao, Y.F.; Ostachowicz, W. Structural Damage Identification Using Damping: A Compendium of Uses and Features. *Smart Mater. Struct.* **2017**, *26*. [CrossRef]
9. Homaei, F.; Shojaee, S.; Ghodrati Amiri, G. A direct damage detection method using Multiple Damage Localization Index Based on Mode Shapes criterion. *Struct. Eng. Mech.* **2014**, *49*, 183–202. [CrossRef]
10. Ravi Prakash Babu, K.; Raghu Kumar, B.; Narayana, K.L.; Mallikarjuna Rao, K. Multiple crack detection in beams from the differences in curvature mode shapes. *J. Eng. Appl. Sci.* **2015**, *10*, 1701–1710.
11. Cao, M.; Radzieński, M.; Xu, W.; Ostachowicz, W. Identification of multiple damage in beams based on robust curvature mode shapes. *Mech. Syst. Signal Process.* **2014**, *46*, 468–480. [CrossRef]
12. Yazdanpanah, O.; Seyedpoor, S.M.; Akbarzadeh Bengar, H. A new damage detection indicator for beams based on mode shape data. *Struct. Eng. Mech.* **2015**, *53*, 725–744. [CrossRef]
13. Rucevskis, S.; Wesolowski, M.; Chate, A. Vibration-Based Damage Identification in Laminated Composite Beams. *Constr. Sci.* **2009**, *10*, 100–112. [CrossRef]
14. Rucevskis, S.; Janeliukstis, R.; Akishin, P.; Chate, A. Mode shape-based damage detection in plate structure without baseline data. *Struct. Control Health Monit.* **2016**, *23*, 1180–1193. [CrossRef]
15. Zhong, S.; Oyadiji, S.O. Crack detection in simply supported beams without baseline modal parameters by stationary wavelet transform. *Mech. Syst. Signal Process.* **2007**, *21*, 1853–1884. [CrossRef]

16. Jaiswal, N.G.; Pande, D.W. Sensitizing the Mode Shapes of Beam Towards Damage Detection Using Curvature and Wavelet Transform. *Int. J. Sci. Technol. Res.* **2015**, *4*, 266–272.

17. Xiang, J.; Liang, M. Wavelet-based detection of beam cracks using modal shape and frequency measurements. *Comput.-Aided Civ. Infrastruct. Eng.* **2012**, *27*, 439–454. [CrossRef]

18. Doebling, S.W.; Farrar, C.R.; Prime, M.B.; Shevitz, D.W. *Damage Identification and Health Monitoring of Structural and Mechanical Systems from Changes in their Vibration Characteristics: A Literature Review*; Los Alamos National Laboratory Report, LA-13070-MS; Los Alamos National Laboratory: Los Alamos, NM, USA, 1996.

19. Lifshitzand, J.M.; Rotem, A. Determination of Reinforcement Unbonding of Composites by a Vibration Technique. *J. Compos. Mater.* **1969**, *3*, 412–423. [CrossRef]

20. Salawu, O.S. Detection of structural damage through changes in frequency: A review. *Eng. Struct.* **1997**, *19*, 718–723. [CrossRef]

21. Dahak, M.; Touat, N.; Benseddiq, N. On the classification of Normalized Natural Frequencies for damage detection in cantilever beam. *J. Sound Vib.* **2017**, *402*, 70–84. [CrossRef]

22. Banerjee, A.; Panigrahi, B.; Pohit, G. Crack modeling and detection in Timoshenko FGM beam under transverse vibration using frequency contour and response surface model with GA. *Nondestruct. Test. Evaluation* **2016**, *31*, 142–164. [CrossRef]

23. Dahak, M.; Touat, N.; Kharoubi, M. Damage detection in beam through change in measured frequency and undamaged curvature mode shape. *Inverse Probl. Sci. Eng.* **2018**. accepted. [CrossRef]

24. Mazanoglu, K.; Sabuncu, M. A frequency based algorithm for identification of single and double cracked beams via a statistical approach used in experiment. *Mech. Syst. Signal Process.* **2012**, *30*, 168–185. [CrossRef]

25. Moradi, S.; Razi, P.; Fatahi, L. On the application of bees algorithm to the problem of crack detection of beam-type structures. *Comput. Struct.* **2011**, *89*, 2169–2175. [CrossRef]

26. Moezi, S.A.; Zakeri, E.; Zare, A.; Nedaei, M. On the application of modified cuckoo optimization algorithm to the crack detection problem of cantilever Euler–Bernoulli beam. *Comput. Struct.* **2015**, *157*, 42–50. [CrossRef]

27. Kaminski, P.C. The approximate location of damage through the analysis of natural frequencies with artificial neural networks". *J. Process Mech. Eng.* **1995**, *209*, 117–123. [CrossRef]

28. Buezas, F.S.; Rosales, M.B.; Filipich, C.P. Damage detection with genetic algorithms taking into account a crack contact model. *Eng. Fract. Mech.* **2011**, *78*, 695–712. [CrossRef]

29. Boubakir, L.; Touat, N.; Kharoubi, M.; Benseddiq, N. Application of improved accelerated random search algorithm for structural damage detection. *Int. J. Acoust. Vib.* **2017**, *22*, 353–368. [CrossRef]

30. Touat, N.; Pyrz, M.; Rechak, S. Accelerated random search method for dynamic FE model updating. *Eng. Comput.* **2007**, *24*, 450–472. [CrossRef]

31. Meirovitch, L. *Fundamentals of Vibrations*; McGraw-Hill Comp, Inc.: New York, NY, USA, 2001.

32. Nahvi, H.; Jabbari, M. Crack detection in beams using experimental modal data and finite element model. *Int. J. Mech. Sci.* **2005**, *47*, 1477–1497. [CrossRef]

33. Tada, H.; Paris, P.; Irwin, G. *The Stress Analysis of Cracks Handbook*; Del Research Corp.: Hellertown, PA, USA, 1973.

34. Habtour, E.; Paulus, M.; Dasgupta, A. Modeling Approach for Predicting the Rate of Frequency Change of Notched Beam Exposed to Gaussian Random Excitation. *Shock Vib.* **2014**, *2014*, 164039. [CrossRef]